

Multipartite stationary entanglement generation in the presence of dipole-dipole interaction in an optical cavity

Azar Vafafard ^{1,*}, Alireza Nourmandipour ^{2,†} and Roberto Franzosi^{3,4,1,‡}

¹*QSTAR and CNR, Istituto Nazionale di Ottica, Largo Enrico Fermi 2, I-50125 Firenze, Italy*

²*Department of Physics, Sirjan University of Technology, 7813733385 Sirjan, Iran*

³*DSFTA, University of Siena, Via Roma 56, 53100 Siena, Italy*

⁴*INFN Sezione di Perugia, I-06123 Perugia, Italy*



(Received 12 February 2022; accepted 17 May 2022; published 25 May 2022)

Engineering a stationary entanglement between atoms or ions placed at small distances is a challenging problem in quantum information science. In this paper, the stationary and dynamics of entanglement in a system of dipole-coupled qubits interacting with a single-mode optical cavity in the strong coupling regime are theoretically investigated. We find that the entanglement in the steady state can be induced and tuned in nonresonance cases by considering the dipole-dipole interaction (DDI) between the qubits. We also point out that the novel measure used in this study can quantify the net multiqubit entanglement in the system. By increasing the DDI intensity, the behavior of the system depends on the number of qubits. Interestingly, with only two qubits, the amounts of steady-state entanglement enhances as the DDI intensity increases. For a system with more than two qubits, we find that DDI in the weak range of intensity plays a constructive role in the entanglement between qubits. However, it could destroy the stationary entanglement as the interaction between qubits intensifies. The entanglement of a system consisting of more than two qubits tends to disappear for an ensemble of qubits with smaller interatomic distances that lead to stronger dipolar interaction between nonadjacent qubits. Finally, we study the atomic population transfer as well as the transmitted spectrum.

DOI: [10.1103/PhysRevA.105.052439](https://doi.org/10.1103/PhysRevA.105.052439)

I. INTRODUCTION

Nowadays, it is well known that quantum entanglement in multipartite systems is one of the crucial resources required for developing quantum technologies such as quantum communication [1,2], quantum cryptography [3], quantum computation [4], quantum metrology [5], quantum imaging [6], etc. Entanglement and decoherence, due to the inevitable coupling of a quantum system with the surrounding environment, are two closely connected phenomena. The creation and manipulation of entangled states for quantum systems exposed to the dissipative surrounding environment is a challenging necessity to be satisfied for most quantum operations.

It is worth noting that three different consequences for entanglement evolution have been predicted [7]: first, a dynamic generation of the entangled states that occur in multiphoton resonances for timescales less than decoherence time; second, entanglement destruction as a result of decoherence with the environment that takes place for timescales between decoherence time and the relaxation time; and third, the generation of steady-state entanglement with the assistance of a driving field in longer times for nonresonances. In recent years, several proposals based on the generation of entangled steady states have been proposed theoretically through engineered

dissipative processes [8–11] and also validated in experiments [12–18]. However, such an amount of stationary entanglement is quite low especially when the number of qubits is more than two [19]. Therefore, it is necessary to look for protocols to control and enhance it [20–22]. In this regard, the system in the study is driven by external fields and coupled to a reservoir, causing a nontrivial nonequilibrium dynamic that results in a highly entangled steady state. Stabilization and quantum control of entanglement can be achieved by engineering the quantum reservoir, the system-reservoir couplings, or the driving protocols [23]. Such realizations have been shown experimentally in various quantum systems like trapped ions [12–14], atomic ensembles [15], and superconducting qubits [16–18].

On the other hand, entangled states of a system with two qubits have been well characterized using a variety of analytical measures of entanglement. So, there has been much interest in both theoretical and experimental studies of the entanglement in bipartite qubit systems in recent years [24–27]. However, the study of the entanglement for multipartite systems with more than two qubits is very constrained by the lack of calculable entanglement measures even for pure states. In fact, introducing a general measure is one of the main tasks to quantify and characterize the exact amount of entanglement between the different constituent parts of a multipartite quantum system. Nevertheless, many different approaches have been defined to classify the multipartite entanglement based on the sum of the bipartite entanglement measures over all the possible bipartitions of the whole quantum system [28,29].

*Corresponding author: azarvafafard@gmail.com

†anourmandip@sirjantech.ac.ir

‡roberto.franzosi@unisi.it

For instance, it has been found that for multiqubit systems, increasing the number of qubits of the system causes a change in the degree of entanglement robustness [30]. Interestingly, in a recent work [31], a measure of entanglement has been proposed based on a distance deriving from an adapted application of the Fubini-study metric, which can be computed for either pure or mixed states of an M -qudit hybrid system. This measure has already been utilized to investigate the dynamics of entanglement between two qubits in a dissipative environment [32].

The opportunity of trapping chains of atoms [33–36] and Wigner crystals [37] in an optical cavity opens a new chapter in the field of quantum optics and quantum information studies. The cavity affects the radiative properties of atoms leading to the cavity-induced atom-atom interactions and collective behaviors. In this regard, the atoms are confined in a deep optical lattice potential that is created by the external classical field, and consequently a chain of two-level qubits is formed along the axis of the cavity [33,34]. The hopping and tunneling of atoms between the different sites are neglected. It is worth noticing that various protocols may be experimentally employed to make a trap array in a cavity to hold the neutral atoms at a constant interatomic distance. Applying an extra cavity pump field resonant to the other cavity frequency is a well-known method of atomic trap generation [33,34]. Alternatively, two laser beams crossing each other in the cavity can make an optical lattice along the cavity.

In this paper, we investigate the steady-state multipartite entanglement and population inversion as well as the transmitted spectrum by considering an arbitrary number of two-level qubits (here, up to five) interacting with a single-mode cavity in the presence of dissipation sources. To be closer to the real system, coupling between the qubits by dipole-dipole interaction with a different coupling strength for each pair is also taken into account. The influence of the detuning between coherent laser field and the cavity and also intensity of dipole-dipole interaction on the interest quantities are demonstrated. First, we show that as the number of qubits increases both the population inversion and entanglement are considerably reduced in the presence of strong DDI. However, in the small range of DDI intensities, where only the nearest qubits have dipolar interaction, the steady states of qubits are highly entangled. In the next step, a comparison in the steady-state entanglement computing with the utilized measure and von Neumann entropy is made that reveals the correspondence of these two measures. Finally, the transmission spectrum of the quantum system will be studied for an ensemble consisting of different number of qubits. We demonstrate that the transmitted spectrum is enhanced for any number of qubits by the increase of DDI intensities.

The rest of the paper is organized as follow: In Sec. II, we present the theoretical model under study. Section III is devoted to the entanglement dynamics of the atomic system. In Sec. IV, we study the atomic population transfer at the stationary state. Section V describes the transmitted spectrum in detail. Finally, we conclude the paper in Sec. VI.

II. THEORETICAL DESCRIPTION

The system under consideration consists of N two-level atoms (qubits) that are placed at a small distance from each

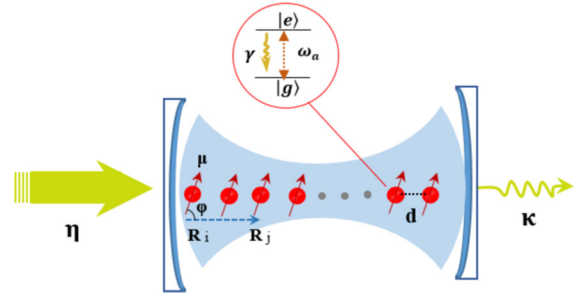


FIG. 1. Schematic diagram of N qubits coupled to each other by dipole-dipole interaction. The cavity is pumped by a coherent laser field with strength η . The decay rates of atoms and cavity field are γ and κ , respectively. The interatomic distance is d and φ denotes the angle between the dipole moment (μ) and atomic position vector (R_i). Each atom can be considered as a two-level system with the ground ($|g\rangle$) and excited ($|e\rangle$) states.

other, leading to the presence of dipole-dipole interaction (see Fig. 1). To model the system, we consider an alignment of N identical dipole-coupled atoms interacting with a single-mode high-finesse optical cavity. Then the system is pumped along the cavity axis by a coherent laser field of frequency ω_p and an effective amplitude η . Each atom in the ensemble is considered as an effective two-level system (qubit) with the ground state $|g\rangle$ and the excited state $|e\rangle$ with a transition frequency ω_a . The effective Hamiltonian describing the dipole-dipole interaction between qubits can be written as [38]

$$H_D = Jd^3 \sum_{i \neq j} \frac{1}{|R_i - R_j|^3} (\sigma_i^- \sigma_j^+ + \sigma_j^- \sigma_i^+), \quad (1)$$

Here, σ_k^+ and σ_k^- are the raising and lowering operators of the k th qubit, and R_i and R_j are the position of the i th and j th qubits with respect to the origin, respectively. The positions R_i are assumed to be in a one-dimensional (1D) array with N sites located at equal distances from each other, i.e., d , which is known as the lattice constant. Therefore, the distance between a pair of qubits can be expressed in terms of the lattice constant, i.e., $R_{ij} = R_i - R_j = d(i - j)$. Furthermore, J is given by

$$J = \frac{3}{4} (\Gamma_0 c^3 / \omega_a^3 d^3) (1 - 3 \cos^2 \varphi), \quad (2)$$

where c is the speed of light, $\Gamma_0 = \frac{k_0^3 \mu^3}{2\pi \epsilon_0 \hbar}$ is the atomic spontaneous emission rate in free space, k_0 denotes the transition wave number, and μ is the dipole moment associated with the transition between the two ground and excited levels. Finally, φ shows the atomic dipole moments with respect to the interatomic axis. Here, it is assumed that the dipole moments of the qubits are parallel to each other and are polarized in the direction perpendicular to the interatomic axis, which in turn results in $\cos \varphi = 0$. Therefore, the DDI intensity depends only on the positions of the two atoms in the cavity.

The dipole-dipole interaction introduced in Eq. (1) reveals the fact that the interaction coupling depends on the relative distance via R_{ij}^{-3} . This means beside the nearest neighbor interaction, the interaction between other qubits have also been taken into account. However, the coupling constant between

farther neighbors falls down as the distance between qubits increases. The Hamiltonian of the system in the rotating wave and dipole approximations is given by ($\hbar = 1$)

$$H = -\Delta_c a^\dagger a - \sum_{k=1}^N \Delta_a \sigma_k^+ \sigma_k^- + \sum_{k=1}^N g(a^\dagger \sigma_k^- + a \sigma_k^+) + H_D + \eta(a + a^\dagger), \quad (3)$$

in which a and a^\dagger are the annihilation and creation operators of the cavity field, respectively. $\Delta_a = \omega_p - \omega_a$ and $\Delta_c = \omega_p - \omega_c$ are the detuning of the transition frequency of the atoms and the cavity field and the laser field frequencies, respectively. The first term in the above Hamiltonian is the free Hamiltonian of the cavity, while the second term represents the qubit-free Hamiltonian. The third term illustrates the interaction between qubits and the cavity field with coupling strength g . Finally, the last term is the pump field.

The unavoidable interaction between any real system with its surrounding environment compels one to consider the dissipative effects via the usual Lindblad form in the Born-Markov approximation [39]. In this regard, the time evolution of the density operator ρ , which describes the dynamics of the system, can be written as ($\hbar = 1$)

$$\begin{aligned} \dot{\rho}(t) = & -i[H, \rho] + \kappa(2a\rho a^\dagger - a^\dagger a\rho - \rho a^\dagger a) \\ & + \sum_{i=1}^N \gamma(2\sigma_i \rho \sigma_i^\dagger - \sigma_i^\dagger \sigma_i \rho - \rho \sigma_i^\dagger \sigma_i) \\ & + \sum_{i \neq j=1}^N \gamma'(2\sigma_i \rho \sigma_j^\dagger - \sigma_i^\dagger \sigma_j \rho - \rho \sigma_i^\dagger \sigma_j). \end{aligned} \quad (4)$$

The first term on the left-hand side of the above equation denotes the coherent evolution of the whole system. The second term describes the coupling of the cavity mode with the environment with the decay rate κ . The third term illustrates the dissipation of the qubits into their local environments with decay rate γ . Finally, the last term shows the qubit-qubit cooperation induced by their coupling with a common reservoir that is determined by γ' [38,40]. This part is taken into account only when the atomic distances are small compared to the radiation wavelength.

It should be noticed that throughout the whole paper, without loss of generality, the value of γ' for the nearest neighbor interactions is $\gamma' = 0.05g$ and for nonadjacent neighbours, this parameter falls down by an order of $\frac{1}{|R_i - R_j|^3}$ [41].

In order to simulate the dynamics of the system, we first write the master equation (4) in the compact form

$$\frac{d\rho(t)}{dt} \equiv \mathcal{L}\rho(t), \quad (5)$$

where \mathcal{L} is a linear map usually called Liouvillian superoperator. The general solution of the presented master equation can be written as [42]

$$\rho(t) = \sum_{k=1}^{N^2+1} c_k e^{\lambda_k t} R_k, \quad (6)$$

where $c_k = \text{Tr}(\rho(0)L_k)$. Here, λ_k are the eigenvalues of the equation $\mathcal{L}(R_k) = \lambda_k R_k$ and $\mathcal{L}^\dagger(L_k) = \lambda_k L_k$ satisfying the orthonormality condition $\text{Tr}(R_k L_{k'}) = \delta_{kk'}$. In order to examine the final state of the system, we solve the equation $\mathcal{L}\rho(t) = 0$ to find the steady-state density operator. It is worth noticing that this general solution does not apply for time-dependent master equations [43].

III. ENTANGLEMENT DYNAMICS

In order to quantify the degree of the multipartite entanglement in the atomic system, we use the very recently defined entanglement distance measure (EDM) [31]:

$$E(\rho(t)) := \sum_{\mu=0}^{M-1} \left[\frac{2(d_\mu - 1)}{d_\mu} - \sum_{k=1}^{d_\mu^2-1} \text{Tr}(\sigma_k^\mu \rho)^2 \right], \quad (7)$$

where M is the number of the subsystems and d_μ is the dimension of the Hilbert space of μ th subsystem. Here, $\rho(t)$ is the time-dependent atomic reduced density operator, $M = N$, and $d_0 = d_1 = 2$. Usually, it is convenient to normalize this measure with respect to the number of subsystems, i.e., $E(\rho(t))/M$. In this regard, the entanglement measure varies between 0 (when the qubits are fully separable) and 1 (when they are maximally entangled), i.e., $0 \leq E(\rho(t))/M \leq 1$. This measure has been proposed based on a distance deriving from an adapted application of the Fubini-study metric, which can be computed for either pure or mixed states of an M -qubit hybrid system.

A. Influence of the number of atoms and dipole-dipole interaction on entanglement

Now, we are in a position to examine the effect of all of the introduced parameters on the multipartite entanglement generation. We are interested in the stationary entanglement. This can be obtained by setting the left hand side of Eq. (4) equal to zero. Figure 2 illustrates the stationary generated entanglement as a function of the Δ_c (i.e., the detuning between the cavity field and the laser field frequencies) and the dipole-dipole interaction intensity J for (a) $N = 2$, (b) $N = 3$, (c) $N = 4$, and (d) $N = 5$ and $\Delta_a = 0$, $\eta = 0.12g$, $\kappa = 0.12g$, and $\gamma = 0.076g$.

It is seen that the entanglement in the steady state can be induced and tuned in nonresonance cases. It is evident that the stationary generated entanglement remarkably depends on the dipole-dipole interaction intensity. First of all, for all values of the number of the qubits in the cavity, for $J = 0$, one observes two peaks of entanglement with equal amplitudes so that they are distributed symmetrically around $\Delta_c = 0$. In Fig. 3, we have plotted the distance between two peaks (in terms of g) in the absence of the dipole-dipole interactions as a function of g for several numbers of qubits in the system. First of all, for a given number of qubits in the cavity, the distance between the two peaks depends linearly on g . It also slightly depends on the number of qubits.

On the other hand, in the presence of DDI, the symmetrical behavior of stationary entanglement disappears. In the case of $N = 2$, as the DDI increases, the left peak becomes higher and approaches $\Delta_c = 0$, while the height of the right peak

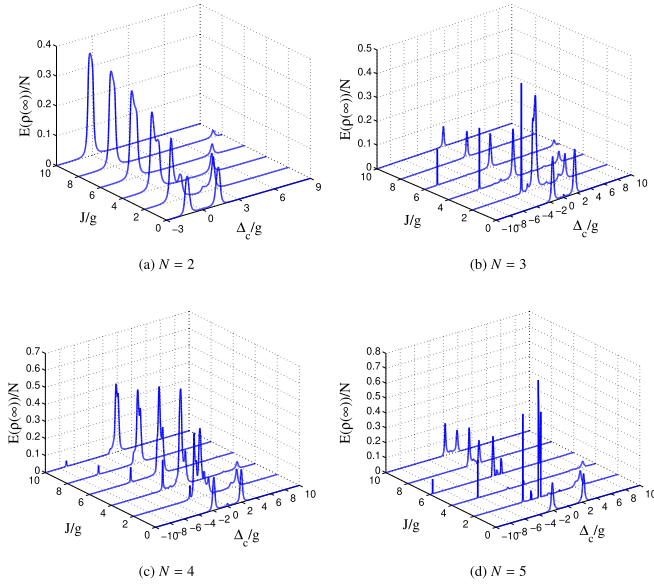


FIG. 2. The normalized stationary generated entanglement as a function of J and Δ_c for (a) $N = 2$, (b) $N = 3$, (c) $N = 4$, and (d) $N = 5$. The other parameters are $\eta = 0.12g$, $\kappa = 0.12g$, and $\gamma = 0.076g$.

is greatly reduced and it departs from $\Delta_c = 0$. This is in agreement with previous studies [44]. Moreover, the distance between the two peaks tends to increase.

For $N > 2$, a different behavior for stationary entanglement is clearly seen. This is due to the fact that the dipolar interaction between nonadjacent qubits contribute to the entanglement in a nonuniform way. See Figs. 2(b)–2(d). Still, for $N > 2$, the qubits decay to a relatively large stationary entangled state in the presence of dipolar interaction at the weak range ($0 \leq J \leq 2g$). For $J > 2g$, the stationary entanglement becomes small. Overall, by comparing the information supplied, one can conclude that the maximum amount of stationary entanglement increases by increasing the number of atoms in the cavity. For instance, for $N = 5$, this value is obtained at $J = 2g$.

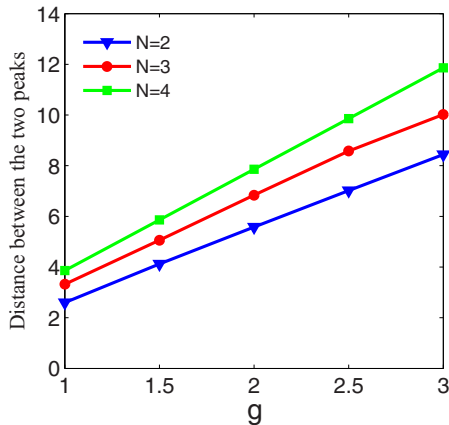


FIG. 3. The distance between two peaks as a function of g for several values of the number of the atoms in the cavity. Other parameters are the same as Fig. 2.

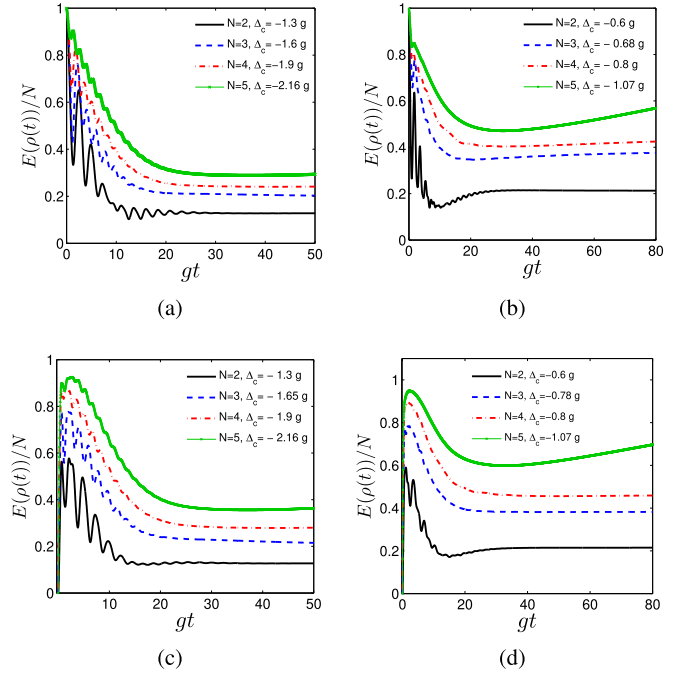


FIG. 4. Dynamics of entanglement as a function of the scaled time $\tau = gt$. Top plots (bottom plots) correspond to initially entangled (ground) state of the qubits. In these plots $J = 0$ (right plots) and $J = 2g$ (left plots). We have chosen the values of Δ_c for which the stationary state could have a peak. Other parameters are the same as in Fig. 2.

Although the stationary entanglement is of great interest, the dynamics of the entanglement could also be important. In Fig. 4, we have illustrated the entanglement dynamics as a function of the scaled time $\tau = gt$ for initially entangled and separable states. We have chosen the values of Δ_c for which the stationary state could have a peak; see Fig. 2. We consider an initially entangled state in which all of the qubits are prepared in an equal superposition of their ground and excited states as follows:

$$|\psi(t=0)\rangle = \frac{1}{\sqrt{2}}(|G\rangle + |E\rangle), \quad (8)$$

in which $|G\rangle$ ($|E\rangle$) means all of the qubits are in their ground (excited) state. In the case of an initially separable state of the system, we consider all of the qubits prepared in their ground state, i.e., $|\psi(t=0)\rangle = |G\rangle$. Furthermore, we assume that the cavity field is initially in the vacuum state.

First of all, it is clear that for an initially separable state, the entanglement starts from zero and increases up to its maximum values and then falls down into its stationary value. This behavior is more or less the same for all of the parameters involved. For small times, an oscillating behavior is clearly seen. It is evident that as the number of the qubits, i.e., N increases, a larger value for the stationary entanglement is observed. This value depends on the DDI intensity, i.e., J : the more values of J , the more stationary entanglement. The interesting aspect here is that, for an initially separable state, it is possible to reach to a nearly maximally entangled state $E(\rho(t))/N \approx 0.95$ at short times.

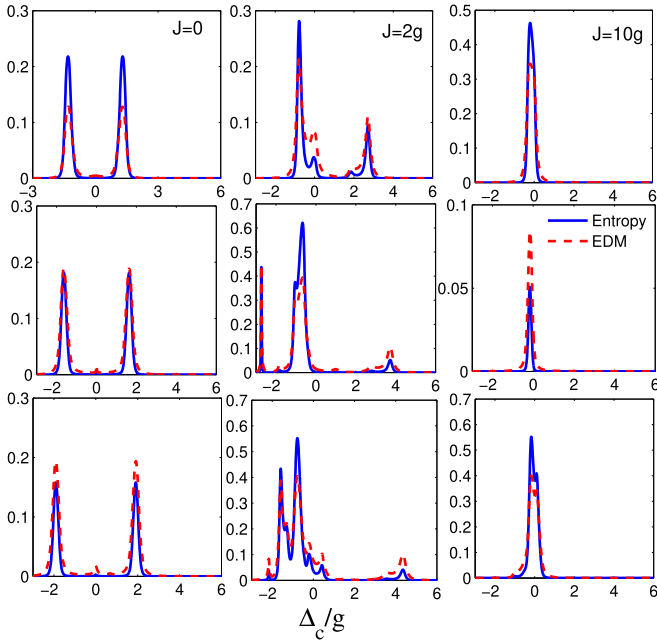


FIG. 5. Comparing the entanglement distance measure (dashed red line) and the von Neumann entropy (solid line) in the stationary state as functions of Δ_c . The first, second, and third columns correspond to $J = 0$, $J = 2g$, and $J = 10g$, respectively. Furthermore, the first, second, and third rows correspond to $N = 2$, $N = 3$, and $N = 4$, respectively. The other parameters are $\Delta_a = 0$, $\eta = 0.12g$, $\kappa = 0.12g$, and $\gamma = 0.076g$.

However, for an initially entangled state, the entanglement starts from its maximum value and decreases as times go on. The oscillatory behavior at shorter times is clearly observed. Again, the stationary entanglement depends on the number of qubits. Also, the effect of the dipole-dipole intensity on the stationary entanglement is quite positive. Furthermore, by comparing these results, it is evident that the stationary entanglement is independent of the initial state of the qubits.

The oscillating behavior of entanglement is due to the non-Markovianity of the process. In this case, the reservoir correlation time is greater than the relaxation time and non-Markovian effects become dominant. In other words, the reservoir feedbacks part of the information which it has captured from the qubit system during the interaction [45].

B. Similarity of the results obtained from the EDM and von Neumann entropy

In Fig. 5, we have compared the stationary entanglement based on entanglement distance (7) and von Neumann entropy, which is computable using the eigendecomposition of the reduced density matrix as follows [46]:

$$S(\rho) = -\sum_i \lambda_i \ln \lambda_i. \quad (9)$$

We find that both the entanglement entropy (solid line) and EDM (dashed line) behave similarly in the presence and absence of DDI. This ensures the validity of using of the entanglement distance measure.

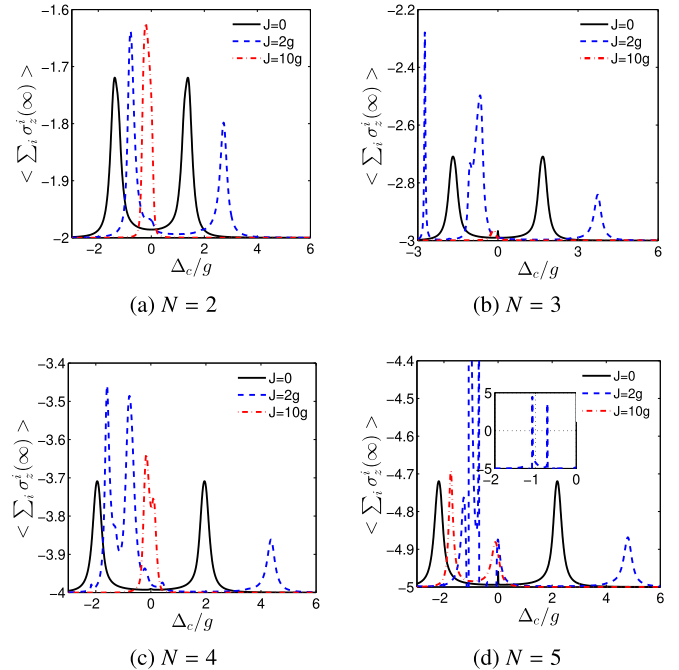


FIG. 6. $\langle S_z \rangle$ at stationary state as a function of Δ_c for several values of J and for (a) $N = 2$, (b) $N = 3$, (c) $N = 4$, and (d) $N = 5$. The other parameters are similar to those in Fig. 2.

IV. ATOMIC POPULATION TRANSFER

It is already known that when a two-level atom interacts with a resonant external field, the atomic population oscillates between the ground and excited states [47]. This mechanism has been used in many applications such as coherent population trapping [48,49], electromagnetically induced transparency [50], chemical dynamics [51], etc.

In this section, we intend to investigate the effect of DDI on the population evolution for several total number of two-level atoms in the cavity. To this end, we calculate the expectation value of the operator $S_z = \sum_{i=1}^N \sigma_z^i$ and depict it versus Δ_c for different values of DDI intensity in Fig. 6. Here we are interested in the stationary state of the system. We notice that the population inversion ranges between $-N$ and N .

First of all, in the absence of dipole-dipole interaction, two peaks with the same amplitude distributed symmetrically around $\Delta_c = 0$ are clearly observed. However, as N increases, the amplitude of these peaks also grows, as is expected. It is very interesting to notice that the distance between these two peaks is quite similar to the stationary entanglement (see Fig. 2). Our further numerical calculations illustrate that behavior of the distance is quite similar to that in Fig. 3. This behavior is more or less the same for all values of the number of qubits in the system.

In the presence of dipole-dipole interaction, for $N = 2$, one observes an increment for the left peak approaching $\Delta_c = 0$, while the opposite behavior is seen for the right peak. However, for $N > 2$ again a different behavior for $\langle S_z \rangle$ is observed. For $0 \leq J \leq 2g$, one observes a relatively large value for $\langle S_z \rangle$, while for $J > 2g$, this value becomes small. The surprising aspect here is that for $N = 5$ and for $J = 2g$ one observes a significant value for the atomic population, i.e., $\langle S_z \rangle \cong 5$.

This means that all of the qubits are nearly excited after the evolution. Overall, there exists great agreement between the population transfer of the qubits and the multipartite entanglement at the stationary state.

It should be noticed that the ability of a global environment in creating stationary entanglement has already been proved in many quantum systems. Here, the results suggest that the global environment is also able to produce a stationary state of simultaneously excited qubits using only one cavity field. The simultaneous excitations of more than two qubits using a single photon has already been predicted theoretically. For instance, in Ref. [52], it has been proved that under specific conditions, one photon can be jointly absorbed by two atoms in their ground state. Moreover, in Ref. [53], it has been predicted that when qubits are placed in different resonators in an array of weakly coupled resonators, the single photon can simultaneously excite more than two qubits. This can be done by storing the initial excitation in a single resonator. Then the excitation is continuously transferred between the nearest-neighbor resonators. Our system can be considered as a generalization of this model, in which, instead of an array of resonators, we have an array of dipolar interacting qubits. The dipolar-dipolar interaction among the qubit system plays the role of the interacting resonator. Therefore, an initial excitation is continuously transferred between the qubits. The interesting aspect here is that the global environment is able to produce not only stationary entanglement but also a stationary state of simultaneously excited qubits.

V. TRANSMITTED SPECTRUM OF ATOMS IN THE CAVITY

In this section, we investigate the transmitted spectrum of the atomic system in detail. To study the spectrum of the coupled atom-cavity system, we use the intracavity photon number $\langle a^\dagger a \rangle$ [54]. Previous studies have shown that for a system of two two-level atoms, the spectrum of the system splits into two resonances which is called the normal-mode or vacuum-Rabi splitting [44]. This is due to the strong coupling regime of the cavity QED. Interestingly, the results reported in this investigation are consistent with our numerical results for $N = 2$. It is possible to illustrate that the effective role of DDI is an atom-cavity detuning which is able to modify the positions and heights of the spectrum peaks [38]. For instance, for $N = 2$, one can show that the effective Hamiltonian becomes [44]

$$H = -\Delta_c a^\dagger a - (\Delta_a - J)\sigma_1^+ \sigma_1^- + \sqrt{2}g(a^\dagger \sigma_1^- + a\sigma_1^+) + \eta(a + a^\dagger). \quad (10)$$

It should be pointed out that for $N > 2$, deriving such an effective Hamiltonian sounds challenging. It is worth noting that in the new representation, the impact of the dipole-dipole interaction is just renormalization of the atomic frequencies. In such a transformed demonstration of Hamiltonian, two fictitious atoms emerge so that only one of them is coupled to the cavity field. In this case, energy exchange with the field occurs through only one of the qubits. In this scenario, the dressed states of the transformed system are similar to those

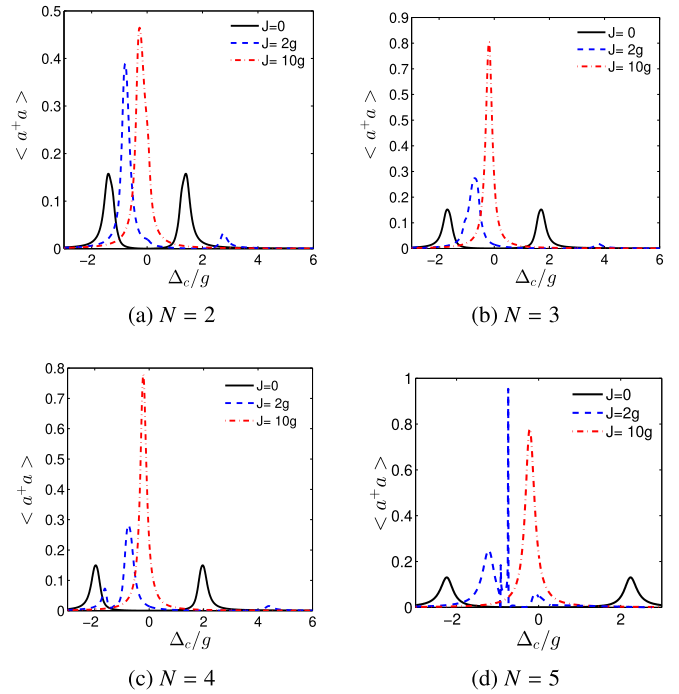


FIG. 7. The normal-mode spectrum for different numbers of qubit (a) $N = 2$, (b) $N = 3$, (c) $N = 4$, and (d) $N = 5$. The other parameters are the same as those in Fig. 2.

of the single-atom system [44],

$$\begin{aligned} |0\rangle &= |g\rangle|0\rangle, \\ |n_-\rangle &= \sin \frac{\theta_n}{2} |e, n-1\rangle - \cos \frac{\theta_n}{2} |g, n\rangle, \\ |n_+\rangle &= \cos \frac{\theta_n}{2} |e, n-1\rangle + \sin \frac{\theta_n}{2} |g, n\rangle, \end{aligned} \quad (11)$$

where $\theta_n = \arctan \frac{2\sqrt{2}g\sqrt{n}}{(\Delta+J)}$ and $\Delta = \omega_a - \omega_c$. The corresponding eigenenergies are

$$\begin{aligned} E_0 &= 0, \\ E_{n\pm} &= \omega_c + \frac{\Delta + J}{2} \pm \frac{1}{2} \sqrt{(\Delta + J)^2 + 8g^2n}. \end{aligned} \quad (12)$$

The spectrum of the first doublet of these states in a degenerate system (for $\omega_a = \omega_c$) splits into two new resonances and is called the normal-mode or vacuum-Rabi splitting.

In Fig. 7, the normal-mode spectrum has been plotted at the stationary state as a function of Δ_c for different numbers of qubits and dipole-dipole interaction coupling. Similar to the stationary multipartite entanglement, one observes that when $J = 0$, there are two peaks with the same amplitude for both resonances and they are symmetrically distributed around $\Delta_c = 0$. It seems that the amplitude of these two peaks is nearly independent of the number of qubits; however, the distance between them increases as N grows. However, in the presence of DDI, the peak appeared in the negative detunings becomes higher and approaches the center by increasing the interaction intensity, while the height of the peak in positive detunings is greatly reduced and it departs from $\Delta_c = 0$. According to what was observed in the entanglement and the population inversion behavior in the absence of DDI, we also

see that the transmitted spectrum of the system is independent of the number of qubits. In the weak DDI regime, more precisely, exactly in the areas where there is an increase in the entanglement and inversion of the population, an increase in the transmitted spectrum also occurs. However, contrary to the findings of the previous two quantities, the transmitted spectrum is amplified by increasing the DDI intensities.

VI. CONCLUDING REMARKS

To sum up, we have studied a model in which an arbitrary number of two-level atoms are interacting with a cavity quantized field in the presence of dissipation sources. We also have considered a dipole-dipole interaction among the two-level systems. Beside the nearest neighbor interactions, the interaction between other qubits have also been taken into account. This is a generalization of a previously studied model in which an arbitrary number of qubits are dissipating into a common environment [55].

In order to quantify the degree of multipartite entanglement, we have used the very recently introduced measure, namely the entanglement distance, which is a powerful tool for quantifying the entanglement of an M -qudit hybrid system [31]. We have studied the validity of the results by comparing them with von Neumann entropy.

We have studied both the stationary and dynamics of multipartite entanglement as a function of Δ_c in the absence and presence of the dipole-dipole interaction. The stationary entanglement is independent of the initial state of the atomic system. In the absence of dipole-dipole interaction, there exist two peaks of entanglement with equal amplitudes which are symmetrically distributed around $\Delta_c = 0$. The distance between these two peaks grows by increasing the atom-field coupling constant g and the number of atoms in the system (see Fig. 3). The presence of dipole-dipole interaction destroys the symmetrical distribution of the peaks of the entanglement. In this scenario, it is found that the behavior of the stationary entanglement differs for $N = 2$ and $N > 2$. For the case $N = 2$, the stationary entanglement increases by increasing the dipole-dipole interaction intensity. However, for $N > 2$, there is an optimal value for J for which the stationary entanglement is maximum. It is evident that this optimal value is around $J = 2g$ for all $N > 2$. For $N = 5$, a nearly maximally entangled state is observed at this value. Furthermore, the dynamics of entanglement has interesting behavior. First of all, from an initially separable state, the entanglement starts from zero up to a maximum value which depends on the number of atoms in the system. For instance, a nearly maximally entangled state, i.e., $E(\rho(t))/N \approx 0.95$ at short times

is observed. Then, we studied the atomic population transfer of the atomic system by computing the expectation value of S_z . It is interesting to point out that the population transfer has a very similar behavior to that of the stationary entanglement. Compare Figs. 2 and 6. It should be noticed that for $N = 5$ and $J = 2g$, a significant value for the atomic population, i.e., $\langle S_z \rangle \cong 5$, is observed. This corresponds to the case in which all of the qubits are excited at the stationary state.

The simultaneous excitation of more than two qubits with a single photon is an interesting behavior in quantum systems. Usually, this process is along with a joint sinusoidal absorption and emission of the single photons. In this paper, we have illustrated numerically that under specific conditions the environment is able to create a stationary state in which all of the qubits are simultaneously excited. This phenomenon can provide useful applications for novel quantum technologies. Furthermore, these results suggest studying the impact of the spatial separation of the qubits on the simultaneous absorption of the single-photon by a collective of qubits. Finally, using the introduced model and its results, one is able to study the nonlinear effects in tight-bonding models in solid state physics, where propagation effects are dominant.

Finally, we have illustrated that the behavior of the transmitted spectrum is slightly different. Similar to what was observed in the entanglement and the population inversion behavior in the absence of DDI, the transmitted spectrum of the system is independent of the number of qubits. In the weak DDI regime, an enhancement of the transmitted spectrum also occurs exactly where there is an increase in the entanglement and inversion of the population. But, contrary to the findings of the previous two quantities, the transmitted spectrum is enhanced even for the strong DDI intensities.

Finally, we should point out that the obtained results are useful in predicting the expected behaviors in actual physical systems where miniaturization of such devices is necessary [12]. Recent studies in practical quantum technologies usually require an array of qubits where interatomic interactions are necessary to be taken into account. Especially in real physical devices, the dissipation is ever present. Therefore, we expect that the presented results could be useful in generating and maybe enhancing the multipartite entanglement.

ACKNOWLEDGMENTS

A.V., A.N., and R.F. acknowledge support by the QuanterA ERA-NET Co-fund 731473 (Project Q-CLOCKS). R.F. acknowledges support by National Group of Mathematical Physics (GNFM-INdAM). A.V. and A.N. are grateful to Girish Saran Agarwal and Ali Morteza pour for extensive discussions.

- [1] D. S. Simon, G. Jaeger, and A. V. Sergienko, *Int. J. Quantum Inform.* **12**, 1430004 (2014).
- [2] G. Brida, M. V. Chekhova, I. P. Degiovanni, M. Genovese, G. K. Kitaeva, A. Meda, and O. A. Shumilkina, *Phys. Rev. Lett.* **103**, 193602 (2009).
- [3] N. Gisin, G. Ribordy, W. Tittel, and H. Zbinden, *Rev. Mod. Phys.* **74**, 145 (2002).

- [4] M. A. Nielsen and I. L. Chuang, *Quantum Computation and Quantum Information* (Cambridge University Press, Cambridge, 2000).
- [5] D. Girolami, A. M. Souza, V. Giovannetti, T. Tufarelli, J. G. Filgueiras, R. S. Sarthour, D. O. Soares-Pinto, I. S. Oliveira, and G. Adesso, *Phys. Rev. Lett.* **112**, 210401 (2014).

- [6] M. Genovese, *J. Opt.* **18**, 073002 (2016).
- [7] A. L. Gramajo, D. Domínguez, and M. J. Sánchez, *Phys. Rev. A* **98**, 042337 (2018).
- [8] B. Kraus, H. P. Büchler, S. Diehl, A. Kantian, A. Micheli, and P. Zoller, *Phys. Rev. A* **78**, 042307 (2008).
- [9] F. Verstraete, M. M. Wolf, and J. I. Cirac, *Nat. Phys.* **5**, 633 (2009).
- [10] F. Reiter, L. Tornberg, G. Johansson, and A. S. Sørensen, *Phys. Rev. A* **88**, 032317 (2013).
- [11] F. Tacchino, A. Auffèves, M. F. Santos, and D. Gerace, *Phys. Rev. Lett.* **120**, 063604 (2018).
- [12] J. T. Barreiro, M. Müller, P. Schindler, D. Nigg, T. Monz, M. Chwalla, M. Hennrich, C. F. Roos, P. Zoller, and R. Blatt, *Nature (London)* **470**, 486 (2011).
- [13] Y. Lin, J. Gaebler, F. Reiter, T. R. Tan, R. Bowler, A. Sørensen, D. Leibfried, and D. J. Wineland, *Nature (London)* **504**, 415 (2013).
- [14] D. Kienzler, H.-Y. Lo, B. Keitch, L. De Clercq, F. Leupold, F. Lindenfelser, M. Marinelli, V. Negnevitsky, and J. Home, *Science* **347**, 53 (2015).
- [15] H. Krauter, C. A. Muschik, K. Jensen, W. Wasilewski, J. M. Petersen, J. I. Cirac, and E. S. Polzik, *Phys. Rev. Lett.* **107**, 080503 (2011).
- [16] S. Shankar, M. Hatridge, Z. Leghtas, K. Sliwa, A. Narla, U. Vool, S. M. Girvin, L. Frunzio, M. Mirrahimi, and M. H. Devoret, *Nature (London)* **504**, 419 (2013).
- [17] Z. Leghtas, U. Vool, S. Shankar, M. Hatridge, S. M. Girvin, M. H. Devoret, and M. Mirrahimi, *Phys. Rev. A* **88**, 023849 (2013).
- [18] M. E. Kimchi-Schwartz, L. Martin, E. Flurin, C. Aron, M. Kulkarni, H. E. Tureci, and I. Siddiqi, *Phys. Rev. Lett.* **116**, 240503 (2016).
- [19] A. Nourmandipour, M. K. Tavassoly, and M. A. Bolorizadeh, *J. Opt. Soc. Am. B* **33**, 1723 (2016).
- [20] M. Rafiee, A. Nourmandipour, and S. Mancini, *Phys. Lett. A* **384**, 126748 (2020).
- [21] F. Nosrati, A. Morteza pour, and R. Lo Franco, *Phys. Rev. A* **101**, 012331 (2020).
- [22] A. Morteza pour and R. Lo Franco, *Sci. Rep.* **8**, 14304 (2018).
- [23] M. Rafiee, A. Nourmandipour, and S. Mancini, *Phys. Rev. A* **94**, 012310 (2016).
- [24] C. A. González-Gutiérrez, R. Román-Ancheyta, D. Espitia, and R. Lo Franco, *Int. J. Quantum Inform.* **14**, 1650031 (2016).
- [25] Z.-X. Man, Y.-J. Xia, and R. L. Franco, *Sci. Rep.* **5**, 13843 (2015).
- [26] B. Bellomo, G. Compagno, R. L. Franco, A. Ridolfo, and S. Savasta, *Phys. Scr.* **T143**, 014004 (2011).
- [27] M. Rafiee, A. Nourmandipour, and S. Mancini, *Phys. Rev. A* **96**, 012340 (2017).
- [28] A. Borrás, A. Plastino, J. Batle, C. Zander, M. Casas, and A. Plastino, *J. Phys. A: Math. Theor.* **40**, 13407 (2007).
- [29] I. D. Brown, S. Stepney, A. Sudbery, and S. L. Braunstein, *J. Phys. A: Math. Gen.* **38**, 1119 (2005).
- [30] C. Simon and J. Kempe, *Phys. Rev. A* **65**, 052327 (2002).
- [31] D. Cocchiarella, S. Scali, S. Ribisi, B. Nardi, G. Bel-Hadj-Aissa, and R. Franzosi, *Phys. Rev. A* **101**, 042129 (2020).
- [32] A. Nourmandipour, A. Vafafard, A. Morteza pour, and R. Franzosi, *Sci. Rep.* **11**, 16259 (2021).
- [33] S. Gupta, K. L. Moore, K. W. Murch, and D. M. Stamper-Kurn, *Phys. Rev. Lett.* **99**, 213601 (2007).
- [34] M. H. Schleier-Smith, I. D. Leroux, H. Zhang, M. A. Van Camp, and V. Vuletić, *Phys. Rev. Lett.* **107**, 143005 (2011).
- [35] A. Kubanek, M. Koch, C. Sames, A. Ourjoumtsev, T. Wilk, P. W. H. Pinkse, and G. Rempe, *Appl. Phys. B* **102**, 433 (2011).
- [36] O. S. Mishina, *New J. Phys.* **16**, 033021 (2014).
- [37] P. F. Herskind, A. Dantan, J. P. Marler, M. Albert, and M. Drewsen, *Nat. Phys.* **5**, 494 (2009).
- [38] S. Nicolosi, A. Napoli, A. Messina, and F. Petruccione, *Phys. Rev. A* **70**, 022511 (2004).
- [39] M. J. Kastoryano, F. Reiter, and A. S. Sørensen, *Phys. Rev. Lett.* **106**, 090502 (2011).
- [40] A. F. Alharbi and Z. Ficek, *Phys. Rev. A* **82**, 054103 (2010).
- [41] C. Qu and A. M. Rey, *Phys. Rev. A* **100**, 041602(R) (2019).
- [42] K. Macieszczak, M. Guță, I. Lesanovsky, and J. P. Garrahan, *Phys. Rev. Lett.* **116**, 240404 (2016).
- [43] A. Norambuena, D. Tancara, and R. Coto, *Eur. J. Phys.* **41**, 045404 (2020).
- [44] Y.-Q. Zhang, L. Tan, and P. Barker, *Phys. Rev. A* **89**, 043838 (2014).
- [45] B. Vacchini, A. Smirne, E.-M. Laine, J. Piilo, and H.-P. Breuer, *New J. Phys.* **13**, 093004 (2011).
- [46] D. Petz, *Entropy, von Neumann, and the von Neumann Entropy* (Springer, Berlin, 2001), pp. 83–96.
- [47] F. Ahmadiouri, M. Hosseini, and F. A. Sarreshtedari, *Int. J. Optics Photon.* **14**, 91 (2020).
- [48] X. Xu, B. Sun, P. R. Berman, D. G. Steel, A. S. Bracker, D. Gammon, and L. Sham, *Nat. Phys.* **4**, 692 (2008).
- [49] A. Vafafard, M. Mahmoudi, and G. S. Agarwal, *Phys. Rev. A* **93**, 033848 (2016).
- [50] M. Fleischhauer, A. Imamoglu, and J. P. Marangos, *Rev. Mod. Phys.* **77**, 633 (2005).
- [51] A. Mitra, I. R. Solá, and H. Rabitz, *Phys. Rev. A* **67**, 043409 (2003).
- [52] L. Garziano, V. Macrì, R. Stassi, O. Di Stefano, F. Nori, and S. Savasta, *Phys. Rev. Lett.* **117**, 043601 (2016).
- [53] L. Garziano, A. Ridolfo, A. Miranowicz, G. Falci, S. Savasta, and F. Nori, *Sci. Rep.* **10**, 21660 (2020).
- [54] I. Schuster, A. Kubanek, A. Fuhrmanek, T. Puppe, P. W. H. Pinkse, K. Murr, and G. Rempe, *Nat. Phys.* **4**, 382 (2008).
- [55] A. Nourmandipour, M. K. Tavassoly, and M. Rafiee, *Phys. Rev. A* **93**, 022327 (2016).